



HAL
open science

Winter climate preconditioning of summer vegetation extremes in the Northern Hemisphere

Mohit Anand, Raed Hamed, Nora Linscheid, Patrícia S. Silva, Julie Andre, Jakob Zscheischler, Freya K. Garry, Ana Bastos

► To cite this version:

Mohit Anand, Raed Hamed, Nora Linscheid, Patrícia S. Silva, Julie Andre, et al.. Winter climate preconditioning of summer vegetation extremes in the Northern Hemisphere. *Environmental Research Letters*, 2024, 19, 10.1088/1748-9326/ad627d . insu-04729835

HAL Id: insu-04729835

<https://insu.hal.science/insu-04729835v1>

Submitted on 10 Oct 2024

HAL is a multi-disciplinary open access archive for the deposit and dissemination of scientific research documents, whether they are published or not. The documents may come from teaching and research institutions in France or abroad, or from public or private research centers.

L'archive ouverte pluridisciplinaire **HAL**, est destinée au dépôt et à la diffusion de documents scientifiques de niveau recherche, publiés ou non, émanant des établissements d'enseignement et de recherche français ou étrangers, des laboratoires publics ou privés.



Distributed under a Creative Commons Attribution 4.0 International License



LETTER • OPEN ACCESS

Winter climate preconditioning of summer vegetation extremes in the Northern Hemisphere

To cite this article: Mohit Anand *et al* 2024 *Environ. Res. Lett.* **19** 094045

View the [article online](#) for updates and enhancements.

You may also like

- [A new data-driven map predicts substantial undocumented peatland areas in Amazonia](#)
Adam Hastie, J Ethan Householder, Eurídice N Honorio Coronado *et al.*
- [Quantifying the relative contributions of three tropical oceans to the western North Pacific anomalous anticyclone](#)
Zhiyuan Lu, Lu Dong, Fengfei Song *et al.*
- [An assessment of recent peat forest disturbances and their drivers in the Cuvette Centrale, Africa](#)
Karimon Nesha, Martin Herold, Johannes Reiche *et al.*

ENVIRONMENTAL RESEARCH
LETTERS

LETTER







Winter climate preconditioning of summer vegetation extremes in the Northern Hemisphere

OPEN ACCESS

RECEIVED
8 February 2024REVISED
4 July 2024ACCEPTED FOR PUBLICATION
12 July 2024PUBLISHED
20 August 2024

Original Content from this work may be used under the terms of the [Creative Commons Attribution 4.0 licence](#).

Any further distribution of this work must maintain attribution to the author(s) and the title of the work, journal citation and DOI.

Mohit Anand^{1,2,*} , Raed Hamed³ , Nora Linscheid⁴, Patrícia S Silva⁵ , Julie Andre^{6,7}, Jakob Zscheischler^{1,2,8} , Freya K Garry⁹  and Ana Bastos^{4,10} ¹ Department of Compound Environmental Risks, Helmholtz Centre for Environmental Research—UFZ, Leipzig, Germany² Technische Universität Dresden, Dresden, Germany³ Department of Water and Climate Risk, Institute for Environmental Studies (IVM), Vrije Universiteit Amsterdam, Amsterdam, The Netherlands⁴ Max Planck Institute for Biogeochemistry, Jena, Germany⁵ Universidade de Lisboa, Faculdade de Ciências, Instituto Dom Luiz, Lisboa, Portugal⁶ Laboratoire de Météorologie Dynamique / Institut Pierre Simon Laplace, ENS—PSL Université, Ecole Polytechnique—Institut Polytechnique de Paris, Sorbonne Université, CNRS, Palaiseau, France⁷ Ecole des Ponts, Champs-sur-Marne, France⁸ Center for Scalable Data Analytics and Artificial Intelligence (ScaDS.AI), Dresden-Leipzig, Germany⁹ Met Office, Fitzroy Road, Exeter EX1 3PB, United Kingdom¹⁰ Institute for Earth System Science and Remote Sensing, Leipzig University, Leipzig, Germany

* Author to whom any correspondence should be addressed.

E-mail: mohit.anand@ufz.de

Keywords: winter climate, leaf area index extremes, legacy effects, vegetation activity, compound events

Abstract

The impact of the spring climate on the Northern Hemisphere's summer vegetation activity and extremes has been extensively researched, but less attention has been devoted to whether and how the winter climate may additionally influence vegetation extremes in the summer. Here, we provide insights into the influence of winter temperature and precipitation on summer vegetation extremes in the Northern Hemisphere. To do this, we identify positive and negative extremes in the summer leaf area index (LAI, a proxy for vegetation activity) and assess winter effects on those extremes using logistic regression at the regional scale. Over a quarter of the regions in the Northern Hemisphere show strong winter climate preconditioning on summer LAI extremes, which is typically stronger for croplands than forests. In regions with strong winter preconditioning, the spring LAI mediates the link between winter climate and summer LAI extremes through the ecological memory in seasonal legacy effects. Our findings suggest that extremely low summer LAI in both croplands and forests is preconditioned by colder and drier winters, while extremely high summer LAI in forests is associated with warmer and wetter winters. For low summer LAI in croplands, warmer winters are associated with an increased likelihood of extremes in mid-latitude regions and a reduced likelihood in high-latitude regions. Consideration of winter preconditioning effects may improve our understanding of inter-annual variability of vegetation activity and support agricultural and land management practitioners in anticipating the detrimental effects of winter on crop yields and forest conditions.

1. Introduction

Global vegetation activity is strongly influenced by the variability in climatic conditions on sub-seasonal to decadal timescales, with the relative importance of temperature, radiation and water availability varying regionally (Ding *et al* 2020, Menzel *et al* 2020). Both the interannual climate variability (Nemani *et al*

2003, Bastos *et al* 2013, Gonsamo *et al* 2016, Zhu *et al* 2017) as well as climatic trends (Peng *et al* 2011, Piao *et al* 2011, 2014, Barichivich *et al* 2013, Fu *et al* 2015, Peñuelas *et al* 2017, Wang *et al* 2018a) directly influence the year-to-year differences in vegetation activity and carbon uptake. Understanding the seasonal predictability of future vegetation growth that emerges from climate variability may also assist agricultural

practitioners with planning and decision-making (e.g. Ogallo *et al* 2000, Bruno Soares 2017, An-Vo *et al* 2021).

Memory in land-surface properties—so-called preconditioning or legacy effects—can contribute to the lagged influence of seasonal climate anomalies. For example, winter precipitation and snowmelt can influence vegetation growth over the next growing season in water-limited regions (Peng *et al* 2010, Chen *et al* 2018). Vegetation activity itself can also mediate seasonal legacy effects, which can result in contrasting impacts throughout the growing season. Vegetation-mediated legacy effects arise, for example, in response to warmer spring temperatures than usual, resulting in increased springtime plant activity (Buermann *et al* 2018). This earlier onset of the growing season causes higher water use and faster water depletion until summer (Wolf *et al* 2016, Lian *et al* 2020, Bastos *et al* 2020a, Li *et al* 2022), with especially severe impacts during warm and dry summers (Bastos *et al* 2020a, Bevacqua *et al* 2021). The spring phenology may also influence autumn senescence timing, although the mechanisms of this relationship are not yet fully understood (Liu *et al* 2016).

While the preconditioning effects of spring warming have been widely studied, the influence of the winter climate on spring and summer vegetation activity is not so well understood. For example, warmer winter temperatures can lead to increased vegetation growth by increasing the water supply from glacial melting (Zhang *et al* 2016). However, warm winters can also have negative effects on plant growth due to the reduction in protective snow cover (Kreyling 2010) and fewer chilling days (Tominaga *et al* 2022). Warm winters that induce an earlier onset of the growing season may increase the risk of frost exposure in the leafing, budding and blossoming stages (Marino *et al* 2011, Bigler and Bugmann 2018), and such events could become more likely under climate change in some regions (Pfleiderer *et al* 2019, Vautard *et al* 2023). Short but extreme warming events have been shown to severely damage sub-Arctic landscapes, leading to considerably reduced summer growth (Bokhorst *et al* 2009).

There is mounting evidence of the influence of winter snow on the timing and productivity of the growing season across the Northern Hemisphere (Wang *et al* 2018b, Kelsey *et al* 2021) and the influence of winter precipitation on net primary productivity during the early growing season in forest–grassland ecosystems (Liu *et al* 2022). Chen *et al* (2018) investigated the preconditioning effects of winter temperature and precipitation on spring vegetation activity across Europe and North America and also found that reduced winter precipitation limited the spring vegetation activity over water-limited regions. In their study, the inclusion of climate information from the

previous season in regression models improved their capability to predict (the normalized difference vegetation index, a proxy for vegetation greenness). In Central Europe, winter teleconnections (including those associated with the North Atlantic Oscillation, the East Atlantic and the Scandinavian Patterns) significantly influence vegetation productivity during the growing season (Bastos *et al* 2016, Gonsamo *et al* 2016, Zhu *et al* 2017). Winter legacy effects may reach beyond the spring season, and compensatory effects across seasons also have to be considered (Buermann *et al* 2018, Bastos *et al* 2020a). To our knowledge, no studies have yet systematically addressed the impact of winter climate on vegetation activity extremes in subsequent summers.

Here, we assess the effect of interannual variability in the winter climate conditions on the vegetation activity extremes in the following summer across the Northern Hemisphere between 1982 and 2020. We use the leaf area index (LAI) as a proxy for vegetation activity and study the effect of winter temperature and precipitation on summer LAI extremes using logistic regression. Our study focuses on sub-continental regions and examines crops and forests separately, given the different controls on phenology, growth and stress responses between these two land cover types (Aspinwall *et al* 2015, Liu *et al* 2021, Miguez-Macho and Fan 2021).

2. Data and methods

2.1. Data

2.1.1. LAI

LAI data for the Northern Hemisphere were obtained from the GLOBMAP global LAI Version 3 product (Liu *et al* 2012). The GLOBMAP LAI combines data from the Moderate Resolution Imaging Spectroradiometer and the Advanced Very High Resolution Radiometer to provide a long-term LAI dataset from 1981 to 2020 at an 8 km spatial horizontal resolution. The LAI temporal resolution was fortnightly from 1981 to 2000 and at eight-day intervals from 2001 onwards. The LAI data were gridded to a spatial resolution of $0.25^\circ \times 0.25^\circ$ using area-weighted averages. In our analysis, we use data from 1982 to 2020.

2.1.2. Climate variables

Climate data were obtained from the European Centre for Medium-Range Weather Forecasts' ERA5 reanalysis (Hersbach *et al* 2020). We use monthly total precipitation (P), temperature at 2 m (T), total column volumetric soil water content and snow depth for the period 1982–2020 over the Northern Hemisphere (25° – 75° North). ERA5 data are provided on a regular lat/lon grid with $0.25^\circ \times 0.25^\circ$ spatial resolution.

2.1.3. Land cover

We use the European Space Agency Land Cover dataset (Santoro *et al* 2017) to quantify the fraction of forest and crop cover for each grid cell. The original land cover classification data are provided at 300 m spatial resolution for the period 1982–2019, and we regrid these data to a 0.25° lat/lon grid using the LC-CCI user tool. We use the lookup table from Poulter *et al* (2015), reproduced in table A1, to classify crop and forest grid cells. We aggregate the classes 10, 20 and 30 to represent cropland, and the classes 40–100 to represent forest. To minimise the influence of land cover changes in our analysis, only locations that are classified as forest or cropland for the entire 38 years are used for further analysis.

2.1.4. Reference regions

To explore the distinct regional dynamics over the Northern Hemisphere, we use the Intergovernmental Panel on Climate Change's (IPCC) Sixth Assessment Report Working Group I reference regions (Iturbide *et al* 2020). Of the 46 land regions, we only consider regions in the Northern Hemisphere and further remove regions if the crop cover or forest cover amounts to less than 100 grid cells. We analyse the vegetation activity of 19 regions in the Northern Hemisphere: 17 regions include both cropland and forest, the Russian Arctic (RAR) region contains only forests, and Eastern Central Asia contains only crops (figure A1). This leads to two different but largely overlapping sets of 18 regions (table A2).

2.2. Data preprocessing

We are interested in analysing how the climate affects the interannual variability of the summer LAI. To do this, we preprocess the data by taking the seasonal average precipitation, temperature, soil moisture, snow depth and LAI for boreal winter (December, January and February), spring (March, April and May) and summer (June, July and August). The seasonal averages are linearly detrended to remove potential long-term trends due to climate change since our interest is in the interannual variability. The detrended data are then standardised to unit variance. We identify high (LAI_{high}) and low (LAI_{low}) summer LAI extremes using the local (pixel-wise) 90th and 10th percentiles of the detrended and standardised seasonal LAI averages. To analyse the trends in the fraction of pixels with extreme LAI for each year, we use the Mann–Kendall non-parametric test (Mann 1945, Kendall 1975).

We separately consider croplands and forest areas in our results, referring to low and high summer LAI extremes for croplands as $\text{LAI}_{\text{low}}^{\text{crop}}$ and $\text{LAI}_{\text{high}}^{\text{crop}}$, and respectively for forest areas as $\text{LAI}_{\text{low}}^{\text{forest}}$ and $\text{LAI}_{\text{high}}^{\text{forest}}$.

2.3. Quantifying winter preconditioning effects

Logistic regression is a suitable method to analyse drivers of extreme impacts (Vogel *et al* 2021, Le Grix *et al* 2023) and specifically preconditioned compound events (Zscheischler *et al* 2020, Bevacqua *et al* 2021, Bastos *et al* 2023). Here, we extend the approach proposed by Bevacqua *et al* (2021) for the study of preconditioning effects of meteorological conditions on LAI extremes.

To quantify the importance of winter preconditioning, we train two separate logistic regression models to predict summer LAI extremes. The first model uses only spring and summer meteorological predictors (temperature and precipitation), while the second model additionally includes winter meteorological predictors. The first model is represented as

$$\mathbb{P}(\text{LAI}_{\text{extreme}} | \setminus w) = \frac{1}{1 + \exp(-X_{\text{extreme}}^w)}$$

$$\text{with } X_{\text{extreme}}^w = \alpha_0 + \alpha_1 T_{\text{su}} + \alpha_2 P_{\text{su}} + \alpha_3 T_{\text{sp}} + \alpha_4 P_{\text{sp}}. \quad (1)$$

Here, T_{su} and T_{sp} correspond to the temperature in summer and spring, and P_{su} and P_{sp} correspond to the precipitation in summer and spring, respectively. Regression coefficients are given by $\alpha_0, \dots, \alpha_4$. Extreme summer LAI is abbreviated as $\text{LAI}_{\text{extreme}}$, where extremes can be low or high. The term $\setminus w$ indicates that winter climate was not included for this particular model. The model is used to predict how likely the occurrence of extreme summer LAI in summer is without considering the influence of winter climate, $\mathbb{P}(\text{LAI}_{\text{extreme}} | \setminus w)$.

The second model additionally includes the winter temperature (T_w) and winter precipitation (P_w) as well as their corresponding regression coefficients α_5 and α_6 :

$$\mathbb{P}(\text{LAI}_{\text{extreme}} | w) = \frac{1}{1 + \exp(-X_{\text{extreme}}^w)}$$

$$\text{with } X_{\text{extreme}}^w = \alpha_0 + \alpha_1 T_{\text{su}} + \alpha_2 P_{\text{su}} + \alpha_3 T_{\text{sp}} + \alpha_4 P_{\text{sp}} + \alpha_5 T_w + \alpha_6 P_w. \quad (2)$$

We train the logistic regression models based on pooled data for cropland and forest pixels separately and for each region. This increases the sample size, allowing us to analyse regional patterns but not sub-regional variability. We further consider LAI_{high} and LAI_{low} separately so that we consider 72 pairs of models for the Northern Hemisphere (two land-cover types, 18 regions, two types of extremes). The sample size N varies per region depending on the number of crop and forest pixels within that region ($N = n_{\text{years}} \times n_{\text{pixels}}$, table A2).

Rearranging the logistic regression equation, $X_{\text{extreme}} = \ln\left(\frac{\mathbb{P}(\text{LAI}_{\text{extreme}})}{1 - \mathbb{P}(\text{LAI}_{\text{extreme}})}\right)$, which are the log odds.

Hence, for interpretation of the fitted model, we take the exponential raised to the power of the coefficient of the logistic regression model as they provide a more direct interpretation with respect to the odds of experiencing an extreme over no extreme, $\frac{IP(LAI_{extreme})}{1-IP(LAI_{extreme})}$; for example, for a unit increase in T_w or P_w and keeping all the other variables fixed, the odds of experiencing an extreme relative to a non-extreme LAI change by e^{α_5} or e^{α_6} , respectively.

The model without winter climate (equation (1)) is a nested model with respect to the model with winter climate (equation (2)), as the latter contains all the parameters of the former as well as the parameters α_5 and α_6 . We therefore test whether including the winter climate significantly improves the prediction of summer LAI extremes using the likelihood ratio test with significance level $\alpha = 0.05$. The likelihood ratio test assesses the goodness of fit of two competing nested statistical models and provides a p -value associated with the null hypothesis that both models are equally good. A low p -value therefore means that the model with more parameters is better than the model with fewer parameters.

Given the very large sample size for each region (table A2), the likelihood ratio test might show significant differences even when the differences in predictability between the models are very small. To rank model differences across regions, we use the Receiver Operating Characteristics curve, which is the plot of the true positive rate against the false positive rate for different threshold settings of a binary classifier. The area under the receiver operating characteristics curve (AUROC) is then a predictive performance metric ranging between 0 and 1, with a value of 0.5 representing prediction by random chance and a value of 1 representing perfect prediction. We quantify the strength of winter preconditioning based on the difference in AUROC between models with winter predictors (AUROC_w) and models without winter predictors (AUROC_{\w}).

For regions with strong winter preconditioning, we further analyse the standardised seasonal averages of anomalies in meteorological variables (i.e. composites) in the years with extreme LAI in summer to complement the interpretation of the results based on the logistic regression coefficients. We create composites from the predictors used in the logistic regression and also consider a few additional variables: winter, spring and summer precipitation, temperature, soil moisture, winter and spring snow depth, and spring LAI. As there is no snow in summer in many of the regions, we exclude summer snow from our analysis. We also exclude winter LAI from our analysis because of the very low vegetation activity in winter in the Northern Hemisphere.

3. Results

3.1. Occurrence of summer LAI extremes

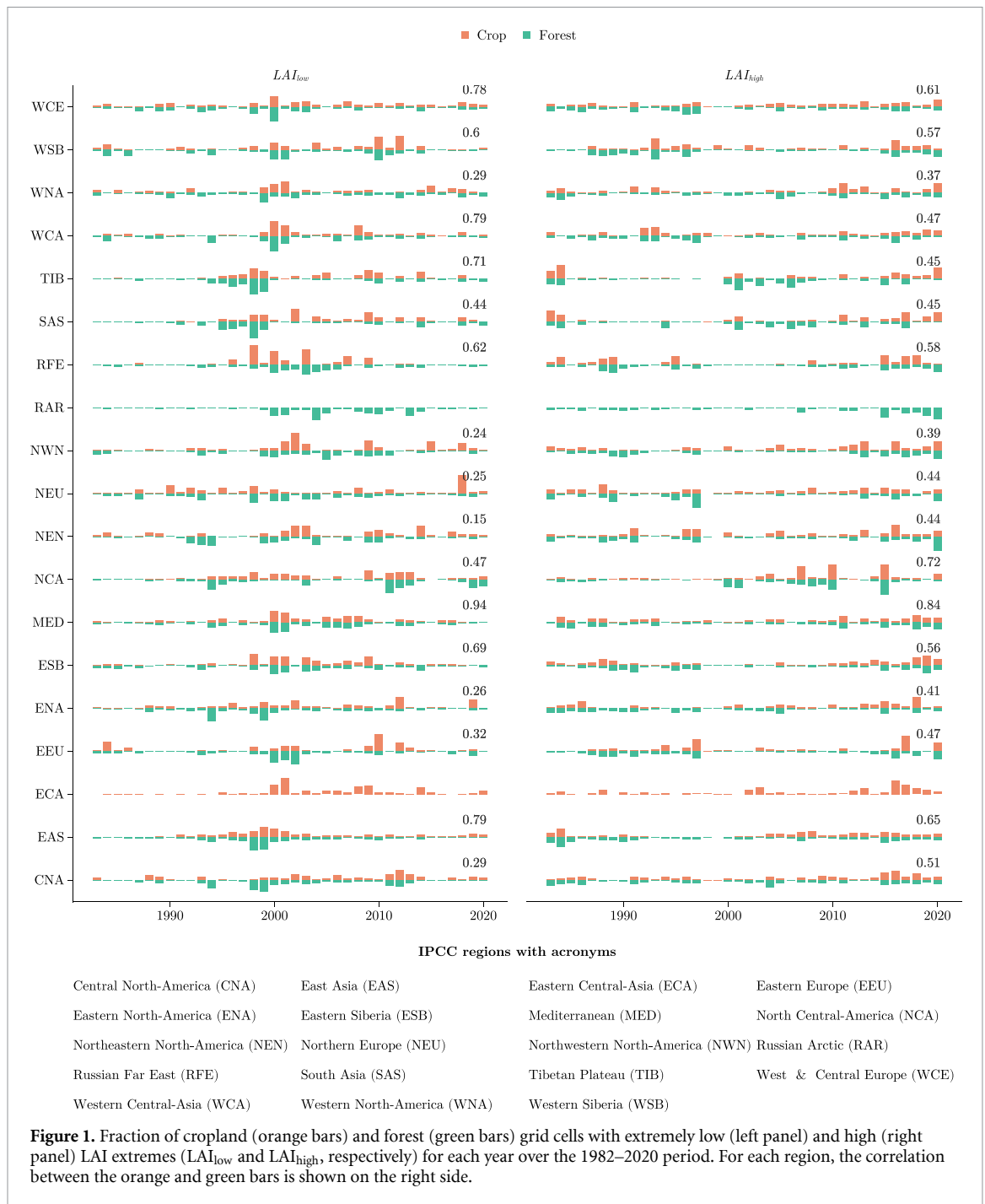
There is large interannual variability in the spatial extent of LAI extremes between 1982 and 2020 for each of the IPCC regions in the Northern Hemisphere (figure 1). Several regions show high temporal correlation between the cropland and forest extents experiencing LAI extremes (numbers in figure 1). The correlation of LAI_{low} between crops and forests tends to reach higher values (seven regions showing correlations above 0.6) than for LAI_{high} (four regions). The Mediterranean (MED) region shows the highest temporal correlation of all regions for both LAI_{low} and LAI_{high}.

Five regions show a significantly increasing trend in the extent of LAI_{low}^{crop}, and ten regions show significantly increasing extents of LAI_{high}^{crop} ($p < 0.05$, table A3). The only region showing a significantly increasing trend ($p < 0.05$) in the extent of LAI_{low}^{forest} is the RAR.

3.2. Preconditioning effect of winter climate on LAI extremes

In general, we find that extremes over cropland are better predicted compared to forests (tables A4 and A5). In all regions, the winter climate significantly improves the prediction of extreme LAI in summers, as determined by the likelihood ratio test of the logistic regression models in equations (1) and (2) ($p < 0.05$). However, despite the effect of the winter climate being significant, in many regions the preconditioning strength is small (overall, AUROC_w minus AUROC_{\w} ranges between 0 and 0.08; tables A4 and A5). For the subsequent analysis, we consider regions with preconditioning strength larger than 0.02 as winter 'preconditioned regions'. This threshold is fixed for all regions and the subjective choice is based on visual investigation of the strength of winter preconditioning for both LAI_{low} and LAI_{high} for crops and forests (figures 2(a), (c), (e) and (g)). This results in five preconditioned regions for both LAI_{low}^{crop} and LAI_{high}^{crop}, eight preconditioned regions for LAI_{low}^{forests}, and five for LAI_{high}^{forests} (figure 2). East Asia (EAS) is the only region where winter preconditioning effects are found for both LAI_{low}^{crop} and LAI_{high}^{crop}. Eastern Siberia (ESB) and RAR are the only regions with high winter preconditioning for both LAI_{low}^{forests} and LAI_{high}^{forests}.

For LAI_{low}, the change in odds ratios associated with P_w (e^{α_6}) is predominantly below 1 across most preconditioned regions for both cropland and forest (figure 3(a), y -axis). This indicates that positive P_w anomalies decrease the odds of LAI_{low} compared to non-extreme summer LAI in these regions. For instance, the decrease in odds of LAI_{low} is more than 40% for Western Central Asia (WCA) for a one



standard deviation increase in P_w over croplands. A notable exception is EAS, where no effect (forests) or the opposite effect (crops) of P_w is observed. In contrast, the effects of T_w (e^{α_5}) are more variable across regions (figure 3(a), x-axis) with the odds of LAI_{low} changing between -35% and $+40\%$ for a one standard deviation increase in T_w . Four regions show positive effects of T_w on LAI_{low} , either in croplands (MED), forests (Central North America (CNA)), or both croplands and forests (EAS, WCA). Two regions show negative T_w effects (Northeastern North America (NEN), Western Siberia (WSB)) for both croplands

and forests, and two regions show negative effects of T_w in forests (Russian Far East (RFE), ESB). These differences largely correspond to background climate conditions: warmer regions (below 40° N) consistently show that positive T_w anomalies increase the odds of LAI_{low} . Conversely, cooler regions (above 40° N) consistently show that positive T_w anomalies decrease the odds of LAI_{low} .

For LAI_{high} , we observe a symmetric effect of T_w , with positive T_w anomalies increasing the odds of LAI_{high} in the northern regions but decreasing them in southern regions (figure 3(b), x-axis). Positive P_w

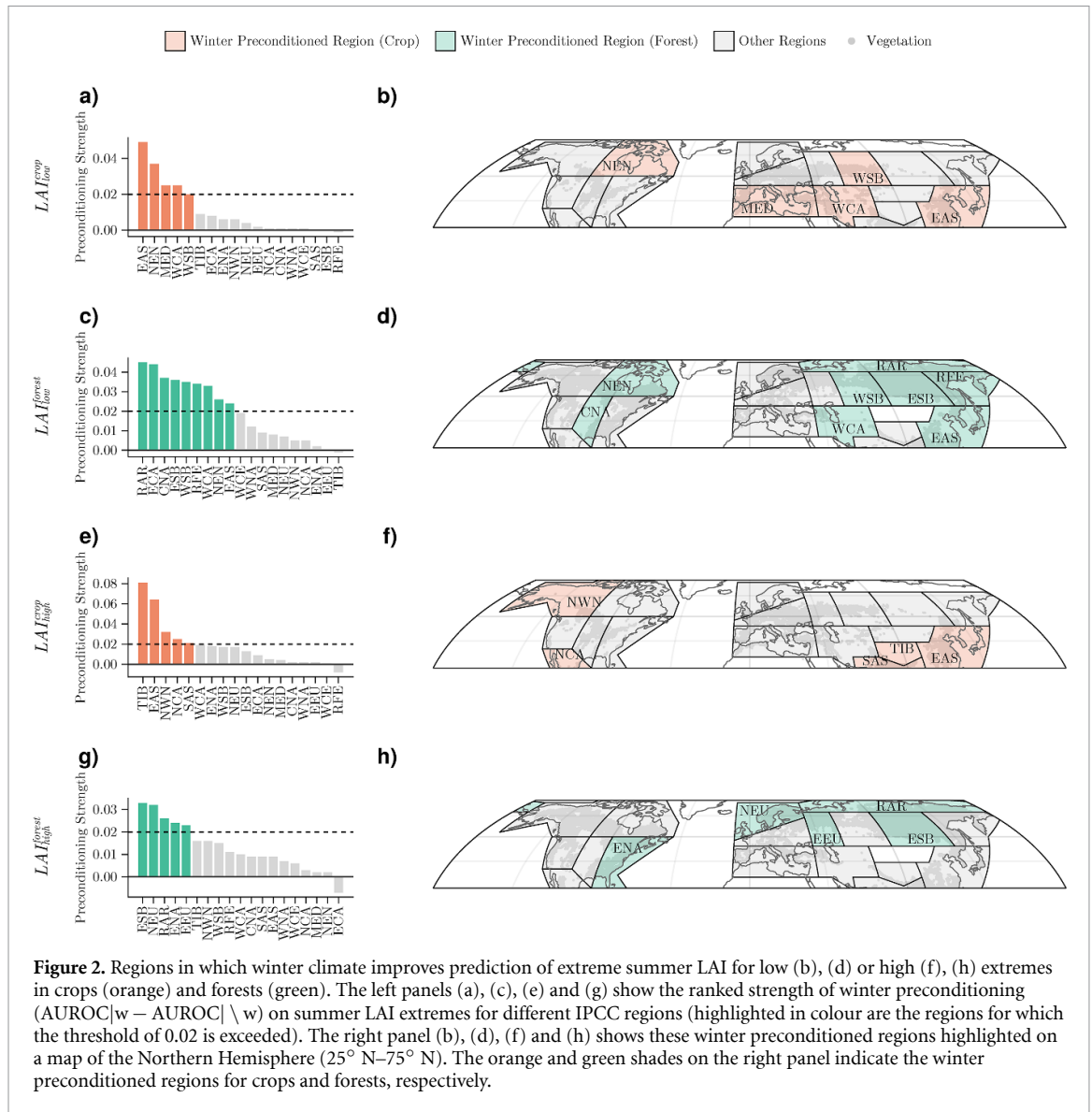
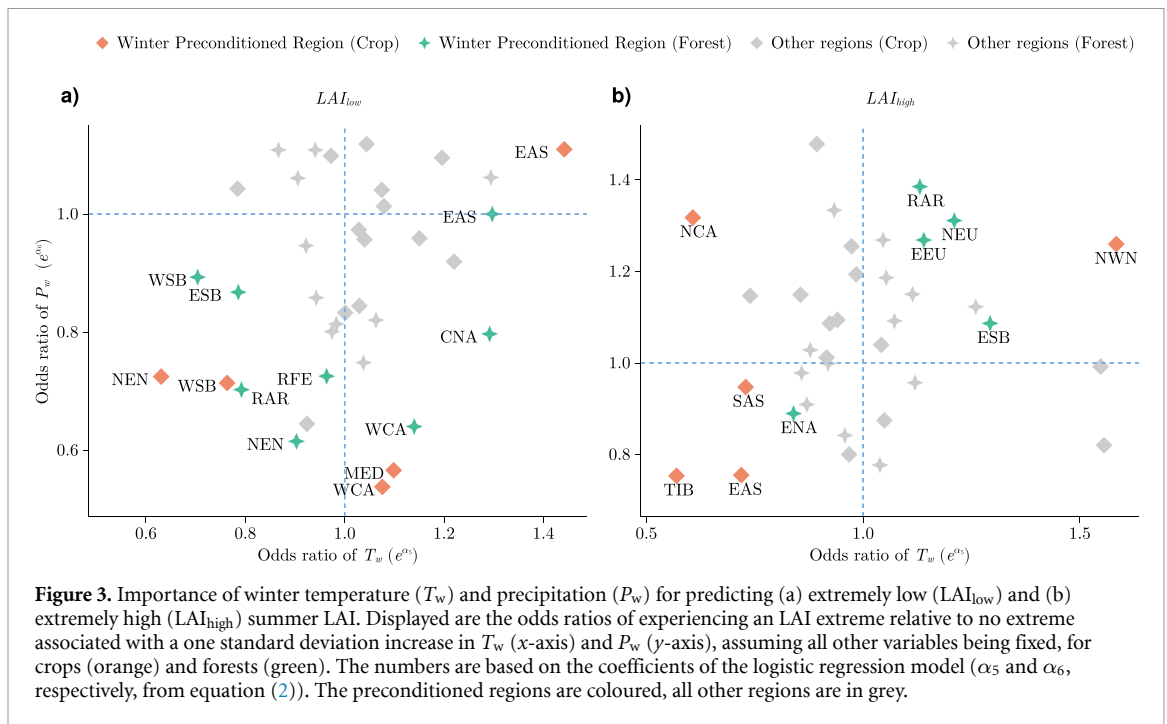


Figure 2. Regions in which winter climate improves prediction of extreme summer LAI for low (b), (d) or high (f), (h) extremes in crops (orange) and forests (green). The left panels (a), (c), (e) and (g) show the ranked strength of winter preconditioning ($AUROC_w - AUROC \setminus w$) on summer LAI extremes for different IPCC regions (highlighted in colour are the regions for which the threshold of 0.02 is exceeded). The right panel (b), (d), (f) and (h) shows these winter preconditioned regions highlighted on a map of the Northern Hemisphere ($25^\circ N-75^\circ N$). The orange and green shades on the right panel indicate the winter preconditioned regions for crops and forests, respectively.

anomalies increase the odds of LAI_{high} in northern regions and decrease them in southern regions, with the exception of crops in North Central America (NCA) that show positive P_w anomalies increase the odds of LAI_{high} (figure 3(b), y -axis). The effect of T_w on the odds ratios of LAI_{high} is stronger than that of P_w , with changes of -43% to 58% for one standard deviation change in T_w , compared to -25% to 38% for P_w .

To understand how relevant the effect of winter is, compared to spring and summer, we compute the odds ratios associated with all predictors for all seasons (tables A6–A9). In many winter preconditioned regions, the effect of a change in T_w is stronger than the effect of a change in the spring or summer climate. This holds for two cropland regions (EAS, NEN) and three forest regions (CNA, WSB, ESB) for LAI_{low} . Similarly, in three crop regions (Northwestern North America (NWN), South Asia (SAS), Tibetan

Plateau (TIB)) and one forest region (ESB), changing T_w leads to the largest change in the odds of LAI_{high} . P_w is affecting the odds of LAI_{low} the most in two regions (MED for croplands and WCA for forests). Even though in some regions neither T_w nor P_w lead to the strongest odds ratio, the effects of winter climate are often stronger than many predictors from spring or summer. For LAI_{low} , P_w is particularly relevant in forests, with seven out of eight regions showing a more strongly reduced odds ratio for P_w than those associated with precipitation in the spring and summer (CNA, ESB, NEN, RAR, RFE, WCA, WSB). Such a strong effect of P_w compared to spring or summer is only found in two out of the five LAI_{low}^{crop} regions (MED, NEN). For LAI_{high} regions, the effect of P_w can be stronger than that of spring (TIB for croplands and Eastern Europe (EEU) for forests), summer (ESB and Northern Europe (NEU) for forests), or spring and summer (EAS for croplands, Eastern North America



(ENA) and RAR for forests) precipitation. Even when T_w is not the most relevant predictor for LAI_{high} (see above), in many regions the effect is still stronger than that of spring (in NCA and EAS croplands and EEU and NEU forests), and stronger than or comparable to that of summer (in ENA forests and EAS croplands, respectively).

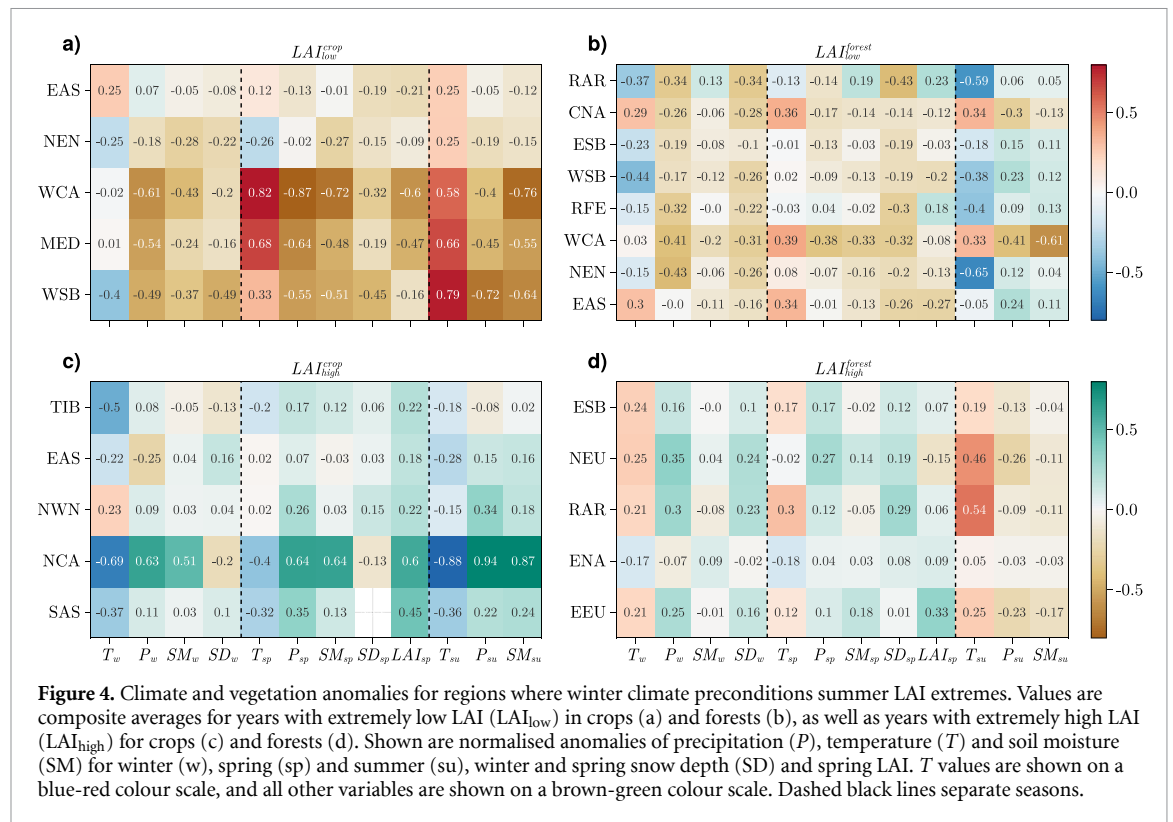
3.3. Direct and indirect climate contributions to summer extremes in winter preconditioned regions

Our analysis reveals that in many regions, winter climate conditions have substantial preconditioning effects on summer LAI extremes. The contribution of a given climatic driver in each season to summer LAI extremes depends not only on the sensitivity of vegetation to the driver but also on the magnitude of the anomalies experienced in those years. Furthermore, for those regions where winter preconditioning effects are relevant, the effects might be direct (e.g. with winter frost leading to vegetation damage) or indirect (e.g. through the winter climate's influence on spring LAI, which then impacts the summer LAI). To further understand the link between winter preconditioning and summer LAI extremes, we quantify the composites of anomalies in T , P and soil moisture in winter, spring and summer; snow depth in winter and spring; and LAI in spring.

Winters corresponding to LAI_{low} in croplands and forests (figures 4(a) and (b)) tend to be drier than average, with predominantly negative anomalies in P_w , SM_w and SD_w . Especially for forests, they also tend to be colder than average (negative T_w

anomalies). The strongest negative T_w anomalies are experienced by WSB (-0.44σ for forests and -0.4σ for croplands), while croplands in WCA, MED and WSB and forests in WCA and NEN show the strongest negative P_w anomalies (below -0.4σ). Exceptions to this pattern are EAS for croplands and forests and CNA for forests, where LAI_{low} is associated with warmer than average winters, and WCA and MED, where T_w anomalies are close to neutral.

In the spring and summer of LAI_{low} years, both croplands and forests show persisting negative anomalies in water-related variables in the spring (precipitation, soil moisture and snow depth), but show opposite anomalies in the summer: croplands are associated with drier and forests with wetter than average conditions for LAI_{low} years. Temperature anomalies are strongly positive in the spring and summer for croplands (except NEN), especially WCA, MED and WSB (with magnitudes $>0.5\sigma$). However, for forests, a switch from normal or warmer-than-average spring conditions to cold summers is found. CNA and WCA are exceptions to this pattern over forests, showing a pattern more consistent with croplands of persisting warmer and drier conditions over spring and summer. In some regions, spring is already associated with lower than average LAI, particularly WCA and MED over croplands and EAS for both croplands and forests. This indicates a potentially indirect effect of winter preconditioning through spring LAI for these regions. However, most regions do not show strongly negative spring LAI anomalies, and RAR even shows positive spring LAI (0.23σ), indicating that winter preconditioning effects on the



negative summer LAI extremes are unlikely to be only due to their effects on spring vegetation activity.

Preconditioned regions with LAI_{high} extremes tend to show opposite patterns for precipitation anomalies in years with LAI_{low} extremes for croplands and forests: most regions experience wetter than average winter and spring conditions, while summer precipitation is above average for croplands and below average for forests. The few exceptions, EAS and NCA for croplands and RAR and ENA for forests, show below-average anomalies in one water-related variable (e.g. SD_w in NCA croplands), but these anomalies are compensated by positive anomalies in the other water-related variables. T_w anomalies are predominantly strong and negative (-0.50σ to -0.22σ) across most preconditioned cropland regions. Unlike croplands, T_w over forest regions is predominantly positive for LAI_{high} extremes (0.21σ – 0.25σ) except ENA (-0.17σ).

The increased water availability during years with LAI_{high} extremes through winter and spring leads to a strong positive LAI anomaly already in the spring for all cropland (0.18σ – 0.60σ) and, less markedly, for most forest regions (0.06σ – 0.33σ) except NEU (-0.15σ). In the summer, as for LAI_{low} , croplands and forest regions show opposing climate anomaly patterns: cropland regions are associated with colder and wetter summers with the exception of TIB, with a small but negative summer precipitation anomaly (-0.08σ); in forest regions LAI_{high} extremes are

associated with drier and warmer conditions in all regions, although the anomalies are small for ENA.

4. Discussion

4.1. Patterns and trends in LAI extremes

Extremes for LAI_{low} tend to co-occur in croplands and forests more than LAI_{high} extremes, possibly because the drivers of LAI_{low} extremes (mostly water limitation) are more consistent between croplands and forests than those of LAI_{high} extremes (figures 3 and 4). However, this could also be due to the relatively coarse resolution of the LAI data ($0.25^\circ \times 0.25^\circ$), which does not allow for full separation of croplands and forests where the land cover heterogeneity is high.

Several regions in the Northern Hemisphere show significant positive trends in the spatial extent of extreme summer LAI over croplands (five regions for LAI_{low}^{crop} and ten for LAI_{high}^{crop}). The positive trends in LAI_{low}^{crop} could be associated with an increase in the spatial extent of compound hot-dry events, e.g. in China (Yang et al 2023), India (Chen et al 2016, Sharma and Mujumdar 2017, Mishra et al 2020), Europe (Manning et al 2019) and in central and western North America (Alizadeh et al 2020). The positive trends in the spatial extent of LAI_{high}^{crop} might be explained by the increased availability of nutrients (through fertilisers and deposition) that contribute to increased crop productivity and growth, especially

during favourable years (Zeng *et al* 2014). For forest regions, the spatial extent of LAI extremes is roughly stable over time (with only one region with a significant trend for LAI_{low}^{forest}). This might be due to the higher resistance of forests to heat and drought stress (Flach *et al* 2018, Xiao *et al* 2023), their longer development times (multi-annual) compared to many croplands (seasonal) as well as the higher diversity in traits influencing their stress responses (Martínez-Vilalta *et al* 2014, Aspinwall *et al* 2015, Anderegg *et al* 2016).

4.2. Winter climate is preconditioning LAI extremes

We show that the winter climate preconditions LAI_{low} and LAI_{high} extremes across large parts of the Northern Hemisphere. In many of the winter preconditioned regions, both high and low extreme summer LAI events are more strongly influenced by winter precipitation and temperature than by spring and summer conditions (tables A6–A9). Odds ratios range from 0.54 to 1.58, indicating an up to 58% change in the odds of occurrence of LAI extremes due to one standard deviation increase in the winter temperature or precipitation. This underscores the critical role of the winter climate in determining extreme summer LAI events, independent of spring and summer weather conditions. Some regions emerge as being particularly sensitive to winter climate conditions: EAS for LAI_{high}^{crop}, LAI_{low}^{crop} and LAI_{low}^{forest}, WCA, WSB and NEN for LAI_{high}^{crop} and LAI_{low}^{crop}, and RAR for LAI_{high}^{forest} and LAI_{low}^{forest}, showing strong winter preconditioning effects.

Similarities between forests and crops are found for low LAI extremes: drier winter conditions generally increase the odds of LAI_{low} (figure 3), and consistently, LAI_{low} extremes are generally preceded by dry winters (figure 4). Among the preconditioned regions, MED and WCA show the strongest sensitivity to winter precipitation and also the strongest negative anomalies in winter precipitation for extreme years. In these regions, summers are typically dry and the growing season starts earlier than in other regions, so drought extremes are more relevant when occurring in the winter and early spring (El-Madany *et al* 2020). Long droughts that span multiple months, including months before planting, have been shown to lead to lower-than-normal yields in various parts of the globe (Zampieri *et al* 2017, Webber *et al* 2018, Santini *et al* 2022). Droughts also have an adverse effect on forest productivity (Park Williams *et al* 2013, Anderegg *et al* 2015, Pohl *et al* 2023, van der Woude *et al* 2023).

Consistent with negative winter precipitation anomalies preceding LAI_{low} extremes, we observe negative snow cover anomalies in the winter, which are still prevalent in the spring in all of the preconditioned regions. Reduced snow cover in winter can lead

to a reduction of soil temperature due to decreased bulk thermal insulation (Henry *et al* 2018, Zhang *et al* 2018). Such conditions have been shown to significantly reduce winter crop productivity by increasing the sensitivity to freezing stress (Trnka *et al* 2014, Zhu *et al* 2019, 2022, Beillouin *et al* 2020). Additionally, the reduced snowpack coupled with below average precipitation in winter results in low soil water availability during the spring (figure 4), inhibiting the development of vegetation at the onset of the growing season (Buermann *et al* 2018, Heino *et al* 2023).

In contrast to the precipitation effects, the temperature effects are more complex, with large variability in the odds of LAI_{low} for both croplands and forests (figure 3), and opposite patterns for crops and forests for LAI_{high}; in forests, warmer winters tend to increase the likelihood of LAI_{high}, and vice versa for croplands. Consistently, the years of LAI_{high}^{crop} are associated with colder than average temperatures, while LAI_{high}^{forest} years show warmer than average temperatures. This is supported by Zscheischler *et al* (2014), who found that low productivity extremes are associated with colder conditions in boreal forests in multiple vegetation models. Overall, higher winter temperatures reduce the risk of frost days, which impedes tree growth and regeneration (Girardin *et al* 2022).

In croplands, the sensitivity of LAI_{low} to winter temperature follows a latitudinal gradient: warmer winters are associated with a higher likelihood of LAI_{low} in mid-latitude regions and a reduced likelihood of LAI_{low} in high-latitude regions. This is supported by a regional study in Sweden, where increased temperatures favoured crop yields in the north but had a negative impact in the south over the period 1965–2020 (Sjulgård *et al* 2023). The relevance of warm winter temperatures for extremely low crop yields has also been highlighted for Europe in previous studies (Ben-Ari *et al* 2018, Beillouin *et al* 2020).

4.3. Winter preconditioning is modulated by spring LAI

In most preconditioned regions, the winter climate effect is already visible in the spring LAI, with similar directions in spring anomalies to those of summer (figure 4). This is consistent with the importance of memory effects in ecological processes (Ogle *et al* 2015, Cranko Page *et al* 2021) and seasonal legacy effects between spring and summer (Buermann *et al* 2018), including for extremes (Wolf *et al* 2016, Bastos *et al* 2020a, Bevacqua *et al* 2021). The climate and spring LAI anomalies in extreme years are generally stronger for crops than forests, reflecting the former's faster response times and also leading to better predictability of extreme years over croplands (tables A4 and A5). The higher predictability over cropland areas may thus be explained by the limited legacy effects of multi-year climate variations

on crops, which are typically annual plants, whereas forest growth and functioning are more likely to show multi-annual legacy effects (Bastos *et al* 2021, Yu *et al* 2022, Cranko Page *et al* 2023a, Anand *et al* 2024). For instance, droughts can have an effect on forest vegetation activity even two years after their occurrence (Yu *et al* 2022), which by far exceeds the nine-month time-span studied here, but could contribute to some variability in the results.

Interestingly, in three snow-dominated regions over forests, we see a reverse direction in the spring LAI anomalies compared to summer LAI anomalies. Specifically, for $LAI_{low}^{forests}$ in RAR and RFE, higher than usual spring LAI (>0.1) anomalies are observed, which might appear counter-intuitive. However, both regions are also associated with low spring snow cover anomalies, aiding in early greening in these years, but are followed by strongly negative summer temperature anomalies (< -0.4) and slightly wetter than average summer conditions. The cold anomalies in the summers, especially for those regions with short growing seasons, might result in damage to the newly budded leaves, leading to $LAI_{low}^{forests}$.

Over NEU for $LAI_{high}^{forests}$, we see a negative anomaly for spring LAI (-0.15σ), but these are followed by warmer and slightly drier summers. As the corresponding spring temperatures are not warmer, vegetation development may only catch up in summers but is favoured by the previous seasons' average moisture. Wang *et al* (2018b) also analysed the impact of snow water equivalent (SWE) in the Northern Hemisphere and found that higher SWE leads to a negative growth effect on vegetation by delaying the snowmelt and reducing the vegetative period, explaining the negative anomalies in the spring LAI. Furthermore, many of these high-latitude regions are typically energy-limited in summer, so colder than average and wetter (i.e. more cloudy) summers tend to be associated with low forest productivity and growth, and the opposite for warm and dry summers (Walther *et al* 2019, Bastos *et al* 2020b).

4.4. Compounding drivers and possible extensions

Large anomalies occur in different variables and seasons, highlighting the compounding nature of the drivers of extreme summer LAI events. For instance, a drier winter followed by a hotter and drier spring and summer typically leads to LAI_{low}^{crop} in WCA, MED and WSB. To fully understand the risks associated with such compound events, multivariate approaches are required that take into account the correlation structure across time and between variables (Ogle *et al* 2021, Cranko Page *et al* 2023a). For instance, Zscheischler *et al* (2017) found that bivariate return periods of precipitation and temperature can well explain crop yields in different European countries. Similarly, using a new index tailored to

bivariate variations in temperature and precipitation, Li *et al* (2022) found that compound warm-dry events increase vegetation productivity at high latitudes, consistent with the fact that these ecosystems are typically energy-limited in the summer. In contrast, such events reduce productivity in the mid-latitudes, and compound warm-dry springs can cause and amplify summer droughts, thereby reducing summer productivity.

Our study provides a first report on the large-scale winter preconditioning effects of summer LAI extremes. However, we note that we do not explore the effects of ecological and human factors in modulating the impacts on LAI (Bastos *et al* 2023). Such modulating factors include regional differences in phenology, the effects of landscape management, irrigation, topography, succession, as well as climate-driven disturbances such as fire or insects (Seidl *et al* 2017). However, we expect that these processes play minor roles at the coarse spatial and temporal resolution considered here. As such, our study lays the basis for more detailed, high-resolution regional analyses. Our approach is anchored in identifying linear relationships with no interactions, which eases the interpretation but with limited predictive skill. Nonlinear approaches based on machine learning can be combined with interpretation techniques to identify drivers of impact extremes (Jiang *et al* 2022, 2024) but require careful model calibration when working with spatiotemporal data (Sweet *et al* 2023). We also do not identify causal relationships between variables. As our results indicate multiple relevant climate anomalies across seasons, chains of weather patterns and their impacts (like droughts and heat waves) should be further studied to identify causal links and carry-over effects across seasons. Such causal links could be investigated using process-based models that simulate the climatic and non-climatic controls for vegetation functioning, structure and dynamics.

5. Conclusions

In this study, we analyse the influence of winter climate on summer LAI extremes for croplands and forests in the Northern Hemisphere. We define winter preconditioning strength based on the ability of the winter climate to improve the prediction of extremes in the summer LAI in comparison to using only spring and summer climate information. Winter preconditioning the occurrence of summer LAI extremes for both crops and forests in more than a quarter of the IPCC Northern Hemisphere regions studied. We find that winter climate anomalies allow a better explanation of summer LAI extremes in many regions, but with importance differences between crops and forests and across regions. Low LAI extremes in summer are typically associated with

colder and drier winter conditions in most regions. More diverse responses are identified for high LAI extremes in summer, with the differences being particularly large between crops and forests. Generally, in forests, high summer LAI extremes are associated with warmer and wetter winters. For crops, we also find that the effect of winter climate on high LAI extremes in summer is dependent on latitude. In many regions, the influence of winter climate is already visible in the spring LAI, highlighting the importance of ecological memory in seasonal legacy effects. Moreover, the observed anomalies in different climate and state variables across different seasons illustrate the compound nature of the drivers of extreme LAI events. In particular, the winter temperature and precipitation precondition the summer LAI through multiple variables (soil moisture, snow depth and LAI) over winter and spring, highlighting the challenges associated with identifying drivers of summer LAI extremes and the importance of ecological memory for impact assessments. Overall, our study presents evidence for lagged climate and ecological effects spanning from winter to summer for many regions in the Northern Hemisphere, and provides a basis for more in-depth studies at the regional scale.

Data availability statement

All datasets that support the findings of this study are openly available. The GLOBMAP global leaf area index data is available on Zenodo at <https://doi.org/10.5281/zenodo.4700264>. ERA5 reanalysis datasets are freely available for download from the Copernicus website (<https://cds.climate.copernicus.eu/>). Landcover data can be downloaded from the ESA Landcover CCI website (<https://www.esa-landcover-cci.org/>).

No new data were created or analysed in this study.

Acknowledgments

The authors thank the DAMOCLES COST Action CA17109, which funded a Compound Events Training School where this work commenced. M A and J Z acknowledge funding from the Helmholtz Initiative and Networking Fund (Young Investigator Group COMPOUNDX, Grant Agreement VH-NG-1537). R H acknowledges funding from the European Union's Horizon 2020 Research and Innovation Programme under Grant Agreement 820712 (RECEIPT). N L, A B, R H and J Z acknowledge funding from the European Union's Horizon 2020 research and innovation programme under Grant Agreement No. 101003469 (XAIDA). P S S was supported by Fundação para a Ciência e a Tecnologia (FCT), Grant Number SFRH/BD/146646/2019. F K G was supported by the Strategic Priority Fund for UK Climate Resilience. The UK Climate Resilience programme was supported by the UK Research and Innovation Strategic Priorities Fund, and was co-delivered by the Met Office and NERC on behalf of UK Research and Innovation partners AHRC, EPSRC and ESRC. The contribution of F K G is subject to © Crown Copyright, Met Office. A B acknowledges funding by the European Union (ERC StG, ForExD, Grant Agreement No. 101039567).

Author contributions

M A, R H, N L, J Z and A B conceptualised the article and defined the methodology. M A wrote the original draft and did the formal analysis. P S S, J A and F K G contributed to the development of the article through discussion in the initial stage. All the authors contributed to the revision of the manuscript. R H and N L contributed equally.

Appendix. Additional figures and tables

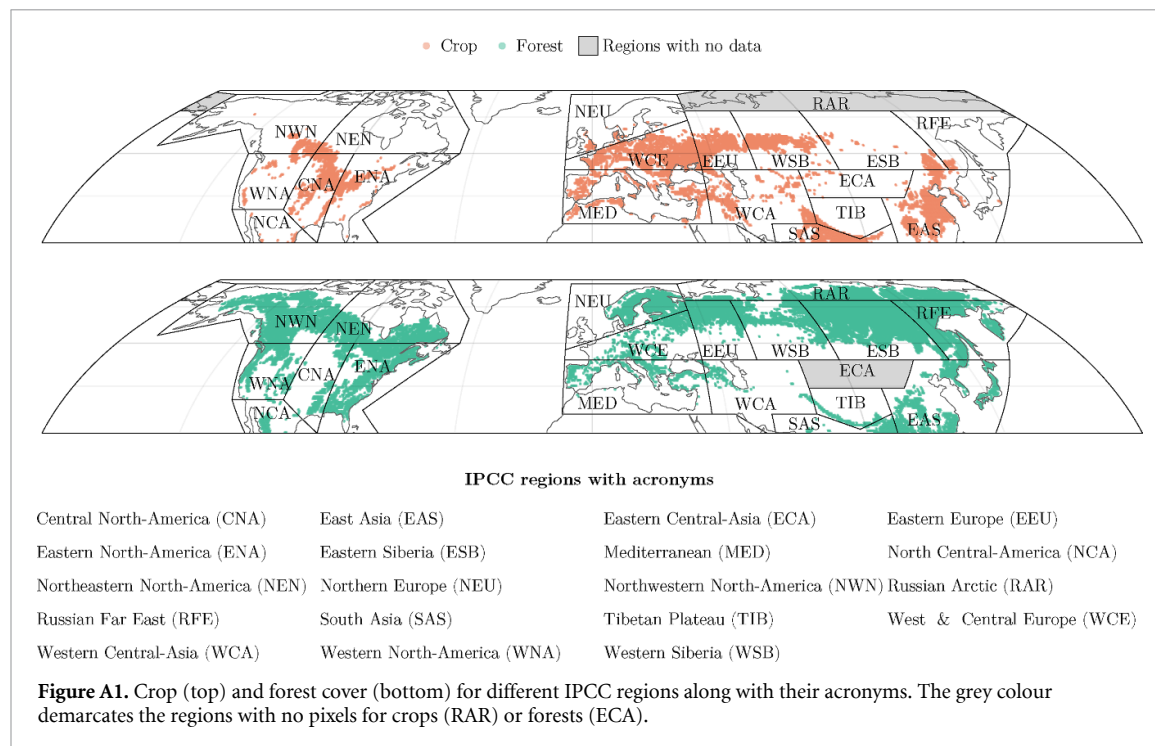


Table A1. Crop vs forest definition in this study.

Class	Description	Type
10	Cropland, rainfed	Crop
20	Cropland, irrigated or post-flooding	Crop
30	Mosaic cropland (>50 % nat. veg. (tree, shrub, herb.) (<50 %)	Crop
40	Mosaic nat. veg. (tree, shrub, herb.) (>50 %)/cropland (<50 %)	Forest
50	Tree cover, broadleaf, evergreen, closed to open (>15 %)	Forest
60	Tree cover, broadleaf, deciduous, closed to open (>15 %)	Forest
70	Tree cover, needleleaf, evergreen, closed to open (>15 %)	Forest
80	Tree cover, needleleaf, deciduous, closed to open (>15 %)	Forest
90	Tree cover, mixed leaf type (broadleaf and needleleaf)	Forest
100	Mosaic tree and shrub (>50 %)/herbaceous cover (<50 %)	Forest

Table A2. Total number of pixels and forest and crop fraction in the IPCC regions.

IPCC region (abbreviation)	Crop fraction (%)	Forest fraction (%)	Total pixels
Central North America (CNA)	33.80	16.95	4944
East Asia (EAS)	20.85	22.98	118 46
Eastern Central Asia (ECA)	3.92	0	4800
Eastern Europe (EEU)	27.92	44.67	6400
Eastern North America (ENA)	9.09	37.27	9638
Eastern Siberia (ESB)	4.60	72.09	128 00
Mediterranean (MED)	16.65	12.35	120 00
North Central America (NCA)	3.55	11.54	2876
Northeastern North America (NEN)	1.25	19.85	192 59
Northern Europe (NEU)	2.58	23.41	142 80
Northwestern North America (NWN)	2.98	32.54	206 72
Russian Arctic (RAR)	0	26.68	235 89
Russian Far East (RFE)	1.13	40.06	121 38
South Asia (SAS)	42.58	19.12	2400
Tibetan Plateau (TIB)	4.58	11.08	3600
Western Central Asia (WCA)	16.28	5.01	9010
Western North America (WNA)	6.63	30.91	5522
Western Siberia (WSB)	16.94	31.13	9600
West & Central Europe (WCE)	52.29	26.26	7720

Table A3. Levels of statistical significance for temporal trends in fractions of pixels with low and high LAI for crop and forest each year, indicated by asterisks and dots. Significance levels: $p < 0.001$ (***), $p < 0.01$ (**), $p < 0.05$ (*), and $p < 0.1$ (·). If trends are significant, they are always increasing.

IPCC region (abbreviation)	LAI _{low} ^{crop}	LAI _{high} ^{crop}	LAI _{low} ^{forest}	LAI _{high} ^{forest}
Central North America (CNA)	*	*		
East Asia (EAS)	·	*		
Eastern Central Asia (ECA)	**	*	NA	NA
Eastern Europe (EEU)				
Eastern North America (ENA)		*		·
Eastern Siberia (ESB)		·		
Mediterranean (MED)		*		
North Central America (NCA)	*	**		
Northeastern North America (NEN)				
Northern Europe (NEU)				
Northwestern North America (NWN)	·	·		
Russian Far East (RFE)				
Russian Arctic (RAR)	NA	NA	*	
South Asia (SAS)	**	**		
Tibetan Plateau (TIB)	*	*		
Western Central Asia (WCA)		*		
Western North America (WNA)				
Western Siberia (WSB)				
West & Central Europe (WCE)	·	*		

Table A4. AUROC curve for the prediction of LAI_{low}. Scores are bold for preconditioned regions.

IPCC region (abbreviation)	Crop ^{\w}	Crop ^w	Forest ^{\w}	Forest ^w
Central North America (CNA)	0.693	0.694	0.616	0.653
East Asia (EAS)	0.577	0.626	0.610	0.634
Eastern Central Asia (ECA)	0.713	0.721	—	—
Eastern Europe (EEU)	0.822	0.824	0.565	0.565
Eastern North America (ENA)	0.636	0.642	0.595	0.597
Eastern Siberia (ESB)	0.703	0.703	0.572	0.608
Mediterranean (MED)	0.793	0.818	0.765	0.773
North Central America (NCA)	0.815	0.816	0.715	0.720
Northeastern North America (NEN)	0.618	0.655	0.726	0.752
Northern Europe (NEU)	0.725	0.729	0.648	0.655
Northwestern North America (NWN)	0.818	0.824	0.704	0.709
Russian Arctic (RAR)	—	—	0.685	0.730
Russian Far East (RFE)	0.714	0.713	0.625	0.659
South Asia (SAS)	0.676	0.676	0.656	0.665
Tibetan Plateau (TIB)	0.623	0.632	0.653	0.652
Western Central Asia (WCA)	0.806	0.831	0.689	0.722
Western North America (WNA)	0.738	0.739	0.636	0.648
Western Siberia (WSB)	0.791	0.811	0.624	0.659
West & Central Europe (WCE)	0.745	0.746	0.608	0.627

Table A5. AUROC curves for the prediction of LAI_{high}. Scores are bold for preconditioned regions.

IPCC region (abbreviation)	Crop ^{\w}	Crop ^w	Forest ^{\w}	Forest ^w
Central North America (CNA)	0.623	0.625	0.583	0.592
East Asia (EAS)	0.587	0.651	0.558	0.567
Eastern Central Asia (ECA)	0.712	0.721	—	—
Eastern Europe (EEU)	0.754	0.756	0.615	0.638
Eastern North America (ENA)	0.648	0.666	0.561	0.585
Eastern Siberia (ESB)	0.664	0.677	0.591	0.624
Mediterranean (MED)	0.795	0.799	0.733	0.735
North Central America (NCA)	0.824	0.849	0.730	0.733
Northeastern North America (NEN)	0.595	0.600	0.681	0.683
Northern Europe (NEU)	0.680	0.697	0.669	0.701
Northwestern North America (NWN)	0.637	0.669	0.645	0.661
Russian Arctic (RAR)	—	—	0.697	0.723
Russian Far East (RFE)	0.566	0.558	0.627	0.638
South Asia (SAS)	0.639	0.660	0.586	0.595
Tibetan Plateau (TIB)	0.596	0.677	0.639	0.655
Western Central Asia (WCA)	0.735	0.754	0.653	0.663
Western North America (WNA)	0.700	0.702	0.633	0.640
Western Siberia (WSB)	0.717	0.734	0.626	0.641
West & Central Europe (WCE)	0.697	0.698	0.585	0.591

Table A6. Odds ratio of different regions for LAI_{low}^{crop}. Winter preconditioned regions are in bold.

IPCC region (abbreviation)	T_w	P_w	T_{sp}	P_{sp}	T_{su}	P_{su}
Central North America (CNA)	1.044	1.119	0.894	0.966	1.499	0.71
East Asia (EAS)	1.442	1.11	0.987	0.828	1.392	1.122
Eastern Central Asia (ECA)	1.196	1.095	1.077	0.45	1.124	0.685
Eastern Europe (EEU)	1.001	0.833	1.679	0.512	1.478	0.553
Eastern North America (ENA)	1.22	0.919	1.046	1.164	1.007	0.682
Eastern Siberia (ESB)	0.784	1.043	1.968	0.779	1.313	0.775
Mediterranean (MED)	1.099	0.566	1.721	0.603	1.448	0.644
North Central America (NCA)	1.079	1.013	1.018	0.472	1.292	0.257
Northeastern North America (NEN)	0.631	0.725	0.818	1.197	1.358	0.868
Northern Europe (NEU)	1.15	0.959	1.395	0.815	1.0	0.528
Northwestern North America (NWN)	0.924	0.645	0.723	0.416	0.975	0.45
Russian Far East (RFE)	0.972	1.099	1.87	0.615	1.738	0.76
South Asia (SAS)	1.04	0.957	1.373	1.097	1.891	1.154
Tibetan Plateau (TIB)	1.029	0.845	1.315	1.176	1.605	1.435
Western Central Asia (WCA)	1.076	0.538	1.336	0.474	1.314	0.71
Western North America (WNA)	1.028	0.973	1.203	0.53	0.971	0.643
Western Siberia (WSB)	0.763	0.714	1.697	0.669	1.401	0.532
West & Central Europe (WCE)	1.075	1.041	1.713	0.687	1.14	0.629

Table A7. Odds ratio of different regions for LAI_{low}^{forest}. Corresponding winter preconditioned regions are in bold.

IPCC region (abbreviation)	T_w	P_w	T_{sp}	P_{sp}	T_{su}	P_{su}
Central North America (CNA)	1.292	0.797	1.208	0.939	1.13	0.836
East Asia (EAS)	1.297	1.0	1.307	1.001	1.067	1.276
Eastern Europe (EEU)	0.941	1.108	1.017	0.946	0.813	0.99
Eastern North America (ENA)	0.906	1.061	1.257	0.813	0.86	1.069
Eastern Siberia (ESB)	0.786	0.868	1.107	0.912	0.801	1.078
Mediterranean (MED)	1.038	0.748	1.815	0.717	1.324	0.659
North Central America (NCA)	0.974	0.801	0.858	0.776	1.988	0.821
Northeastern North America (NEN)	0.903	0.615	1.476	0.862	0.434	0.928
Northern Europe (NEU)	1.063	0.82	0.962	0.808	0.625	0.985
Northwestern North America (NWN)	0.943	0.858	1.05	0.755	0.448	0.78
Russian Arctic (RAR)	0.792	0.703	1.073	0.824	0.475	0.897
Russian Far East (RFE)	0.964	0.725	0.975	1.007	0.599	0.911
South Asia (SAS)	0.867	1.108	1.575	1.085	1.186	1.611
Tibetan Plateau (TIB)	0.922	0.946	1.242	0.985	1.084	1.613
Western Central Asia (WCA)	1.14	0.64	1.261	0.705	1.129	0.702
Western North America (WNA)	0.983	0.814	1.006	0.62	0.889	1.069
Western Siberia (WSB)	0.704	0.893	1.146	0.905	0.725	1.08
West & Central Europe (WCE)	1.294	1.062	1.121	0.766	0.955	1.063

Table A8. Odds ratio of different regions for LAI_{high}^{crop}. Corresponding winter preconditioned regions are in bold.

IPCC region (abbreviation)	T_w	P_w	T_{sp}	P_{sp}	T_{su}	P_{su}
Central North America (CNA)	0.916	1.012	1.163	0.977	0.9	1.441
East Asia (EAS)	0.719	0.755	1.125	1.153	0.716	1.077
Eastern Central Asia (ECA)	0.856	1.149	1.053	1.706	0.914	1.557
Eastern Europe (EEU)	0.923	1.087	0.647	1.8	0.614	1.334
Eastern North America (ENA)	0.739	1.147	1.186	0.813	1.155	1.59
Eastern Siberia (ESB)	0.968	0.8	1.002	1.433	0.798	1.493
Mediterranean (MED)	0.973	1.255	0.601	1.704	0.618	1.37
North Central America (NCA)	0.607	1.318	1.293	1.667	0.461	1.707
Northeastern North America (NEN)	0.984	1.194	0.936	1.004	1.307	1.354
Northern Europe (NEU)	1.556	0.82	0.487	1.198	0.733	1.285
Northwestern North America (NWN)	1.584	1.26	0.783	1.283	0.819	1.39
Russian Far East (RFE)	1.049	0.875	1.09	0.961	1.201	0.983
South Asia (SAS)	0.729	0.947	0.938	1.223	0.736	1.071
Tibetan Plateau (TIB)	0.569	0.754	1.001	1.171	0.823	0.753
Western Central Asia (WCA)	0.893	1.478	0.864	1.642	0.784	1.231
Western North America (WNA)	1.042	1.04	0.81	1.545	0.996	1.464
Western Siberia (WSB)	1.548	0.992	0.671	1.05	0.788	1.817
West & Central Europe (WCE)	0.941	1.094	0.651	1.35	0.791	1.34

Table A9. Odds ratio of different regions for LAI_{high}^{forest}. Corresponding winter preconditioned regions are in bold.

IPCC region (abbreviation)	T_w	P_w	T_{sp}	P_{sp}	T_{su}	P_{su}
Central North America (CNA)	0.858	0.978	0.9	0.966	0.936	1.306
East Asia (EAS)	0.87	0.909	0.924	1.111	1.102	0.933
Eastern Europe (EEU)	1.14	1.269	1.022	1.061	1.269	0.768
Eastern North America (ENA)	0.839	0.89	0.805	1.011	1.115	0.984
Eastern Siberia (ESB)	1.293	1.087	1.117	1.198	1.25	0.962
Mediterranean (MED)	1.073	1.092	0.658	1.412	0.67	1.366
North Central America (NCA)	0.958	0.842	0.845	1.37	0.514	1.247
Northeastern North America (NEN)	0.878	1.028	0.676	1.245	1.95	1.247
Northern Europe (NEU)	1.21	1.311	0.862	1.323	1.782	0.993
Northwestern North America (NWN)	0.933	1.334	0.891	1.309	1.718	1.288
Russian Arctic (RAR)	1.131	1.385	1.307	1.124	2.05	1.058
Russian Far East (RFE)	1.053	1.186	1.215	0.978	1.476	0.95
South Asia (SAS)	1.12	0.957	1.02	1.228	0.888	0.742
Tibetan Plateau (TIB)	1.039	0.777	0.745	1.061	0.731	0.707
Western Central Asia (WCA)	1.046	1.269	0.94	1.175	0.715	1.244
Western North America (WNA)	1.114	1.15	0.81	1.369	0.998	1.111
Western Siberia (WSB)	1.26	1.123	1.091	0.94	1.473	0.962
West & Central Europe (WCE)	0.919	0.999	0.851	1.203	0.931	0.993

ORCID iDs

Mohit Anand  <https://orcid.org/0000-0002-1688-263X>

Raed Hamed  <https://orcid.org/0000-0003-2243-3109>

Patrícia S Silva  <https://orcid.org/0000-0003-0410-2971>

Freya K Garry  <https://orcid.org/0000-0002-9640-6675>

Ana Bastos  <https://orcid.org/0000-0002-7368-7806>

References

- Alizadeh M R, Adamowski J, Nikoo M R, AghaKouchak A, Dennison P and Sadegh M 2020 A century of observations reveals increasing likelihood of continental-scale compound dry-hot extremes *Sci. Adv.* **6** eaaz4571
- An-Vo D-A, Radanielson A M, Mushtaq S, Reardon-Smith K and Hewitt C 2021 A framework for assessing the value of seasonal climate forecasting in key agricultural decisions *Clim. Serv.* **22** 100234
- Anand M, Bohn F J, Camps-Valls G, Fischer R, Huth A, Sweet L-B and Zscheischler J 2024 Identifying compound weather drivers of forest biomass loss with generative deep learning *Environ. Data Sci.* **3** e4
- Anderegg W R L et al 2015 Pervasive drought legacies in forest ecosystems and their implications for carbon cycle models *Science* **349** 528–32
- Anderegg W R L, Klein T, Bartlett M, Sack L, Pellegrini A F A, Choat B and Jansen S 2016 Meta-analysis reveals that hydraulic traits explain cross-species patterns of drought-induced tree mortality across the globe *Proc. Natl Acad. Sci.* **113** 5024–9
- Aspinwall M J, Loik M E, Resco De Dios V, Tjoelker M G, Payton P R and Tissue D T 2015 Utilizing intraspecific variation in phenotypic plasticity to bolster agricultural and forest productivity under climate change *Plant Cell Environ.* **38** 1752–64
- Barichivich J, Briffa K R, Myneni R B, Osborn T J, Melvin T M, Ciais P, Piao S and Tucker C 2013 Large-scale variations in the vegetation growing season and annual cycle of atmospheric CO₂ at high northern latitudes from 1950 to 2011 *Glob. Change Biol.* **19** 3167–83
- Bastos A et al 2016 European land CO₂ sink influenced by NAO and East-Atlantic pattern coupling *Nat. Commun.* **7** 10315
- Bastos A et al 2020a Direct and seasonal legacy effects of the 2018 heat wave and drought on European ecosystem productivity *Sci. Adv.* **6** eaba2724
- Bastos A et al 2020b Impacts of extreme summers on European ecosystems: a comparative analysis of 2003, 2010 and 2018 *Phil. Trans. R. Soc. B* **375** 20190507
- Bastos A et al 2021 Increased vulnerability of European ecosystems to two compound dry and hot summers in 2018 and 2019 *Earth Syst. Dyn.* **12** 1015–35
- Bastos A, Running S W, Gouveia C and Trigo R M 2013 The global NPP dependence on ENSO: La Niña and the extraordinary year of 2011 *J. Geophys. Res. Biogeosci.* **118** 1247–55
- Bastos A, Sippel S, Frank D, Mahecha M D, Zaehle S, Zscheischler J and Reichstein M 2023 A joint framework for studying compound ecoclimatic events *Nat. Rev. Earth Environ.* **4** 333–50
- Beillouin D, Schauburger B, Bastos A, Ciais P and Makowski D 2020 Impact of extreme weather conditions on European crop production in 2018 *Phil. Trans. R. Soc. B* **375** 20190510
- Ben-Ari T, Boé J, Ciais P, Lecerf R, Van der Velde M and Makowski D 2018 Causes and implications of the unforeseen 2016 extreme yield loss in the breadbasket of France *Nat. Commun.* **9** 1627
- Bevacqua E et al 2021 Guidelines for studying diverse types of compound weather and climate events *Earth's Future* **9** e2021EF002340
- Bigler C and Bugmann H 2018 Climate-induced shifts in leaf unfolding and frost risk of European trees and shrubs *Sci. Rep.* **8** 9865
- Bokhorst S F, Bjerke J W, Tømmervik H, Callaghan T V and Phoenix G K 2009 Winter warming events damage sub-Arctic vegetation: consistent evidence from an experimental manipulation and a natural event *J. Ecol.* **97** 1408–15
- Bruno Soares M 2017 Assessing the usability and potential value of seasonal climate forecasts in land management decisions in the southwest UK: challenges and reflections *Adv. Sci. Res.* **14** 175–80
- Buermann W et al 2018 Widespread seasonal compensation effects of spring warming on northern plant productivity *Nature* **562** 110–4

- Chen C, He B, Guo L, Zhang Y, Xie X and Chen Z 2018 Identifying critical climate periods for vegetation growth in the northern hemisphere *J. Geophys. Res. Biogeosci.* **123** 2541–52
- Chen Y, Zhang Z, Wang P, Song X, Wei X and Tao F 2016 Identifying the impact of multi-hazards on crop yield—a case for heat stress and dry stress on winter wheat yield in northern China *Eur. J. Agron.* **73** 55–63
- Cranko Page J, De Kauwe M G, Abramowitz G, Cleverly J, Hinko-Najera N, Hovenden M J, Liu Y, Pitman A J and Ogle K 2021 Examining the role of environmental memory in the predictability of carbon and water fluxes across Australian ecosystems *Biogeosciences* **19** 1913–32
- Cranko Page J, De Kauwe M G, Abramowitz G and Pitman A J 2023a Non-stationary lags and legacies in ecosystem flux response to antecedent rainfall *J. Geophys. Res. Biogeosci.* **128** e2022JG007144
- Ding Y, Li Z and Peng S 2020 Global analysis of time-lag and-Accumulation effects of climate on vegetation growth *Int. J. Appl. Earth Obs. Geoinf.* **92** 102179
- El-Madany T S, Carrara A, Martín M P, Moreno G, Kolle O, Pacheco-Labrador J, Weber U, Wutzler T, Reichstein M and Migliavacca M 2020 Drought and heatwave impacts on semi-arid ecosystems' carbon fluxes along a precipitation gradient *Phil. Trans. R. Soc. B* **375** 20190519
- Flach M, Sippel S, Gans F, Bastos A, Brenning A, Reichstein M and Mahecha M D 2018 Contrasting biosphere responses to hydrometeorological extremes: revisiting the 2010 western Russian heatwave *Biogeosciences* **15** 6067–85
- Fu Y H et al 2015 Declining global warming effects on the phenology of spring leaf unfolding *Nature* **526** 104–7
- Girardin M P, Guo X J, Gervais D, Metsaranta J, Campbell E M, Arsenault A, Isaac-Renton M and Hogg E H 2022 Cold-season freeze frequency is a pervasive driver of subcontinental forest growth *Proc. Natl Acad. Sci.* **119** e2117464119
- Gonsamo A, Chen J M and Lombardozzi D 2016 Global vegetation productivity response to climatic oscillations during the satellite era *Glob. Change Biol.* **22** 3414–26
- Heino M, Kinnunen P, Anderson W, Ray D K, Puma M J, Varis O, Siebert S and Kumm M 2023 Increased probability of hot and dry weather extremes during the growing season threatens global crop yields *Sci. Rep.* **13** 3583
- Henry H A L et al 2018 Increased soil frost versus summer drought as drivers of plant biomass responses to reduced precipitation: results from a globally coordinated field experiment *Ecosystems* **21** 1432–44
- Hersbach H et al 2020 The ERA5 global reanalysis *Q. J. R. Meteorol. Soc.* **146** 1999–2049
- Iturbide M et al 2020 An update of IPCC climate reference regions for subcontinental analysis of climate model data: definition and aggregated datasets *Earth Syst. Sci. Data* **12** 2959–70
- Jiang S, Bevacqua E and Zscheischler J 2022 River flooding mechanisms and their changes in Europe revealed by explainable machine learning *Hydrol. Earth Syst. Sci.* **26** 6339–59
- Jiang S, Tarasova L, Yu G and Zscheischler J 2024 Compounding effects in flood drivers challenge estimates of extreme river floods *Sci. Adv.* **10** ead14005
- Kelsey K C, Pedersen S H, Leffler A J, Sexton J O, Feng M and Welker J M 2021 Winter snow and spring temperature have differential effects on vegetation phenology and productivity across Arctic plant communities *Glob. Change Biol.* **27** 1572–86
- Kendall M G 1975 *Rank Correlation Methods* (Griffin)
- Kreyling J 2010 Winter climate change: a critical factor for temperate vegetation performance *Ecology* **91** 1939–48
- Le Grix N, Cheung W L, Reygondeau G, Zscheischler J and Frölicher T L 2023 Extreme and compound ocean events are key drivers of projected low pelagic fish biomass *Glob. Change Biol.* **29** 6478–92
- Li J, Bevacqua E, Chen C, Wang Z, Chen X, Myneni R B, Wu X, Xu C-Y, Zhang Z and Zscheischler J 2022 Regional asymmetry in the response of global vegetation growth to springtime compound climate events *Commun. Earth Environ.* **3** 123
- Lian X et al 2020 Summer soil drying exacerbated by earlier spring greening of northern vegetation *Sci. Adv.* **6** eaax0255
- Liu Q, Fu Y H, Zhu Z, Liu Y, Liu Z, Huang M, Janssens I A and Piao S 2016 Delayed autumn phenology in the northern hemisphere is related to change in both climate and spring phenology *Glob. Change Biol.* **22** 3702–11
- Liu X, Tian Y, Liu S, Jiang L, Mao J, Jia X, Zha T, Zhang K, Wu Y and Zhou J 2022 Time-lag effect of climate conditions on vegetation productivity in a temperate forest–grassland ecotone *Forests* **13** 1024
- Liu Y, Konings A G, Kennedy D and Gentile P 2021 Global coordination in plant physiological and rooting strategies in response to water stress *Glob. Biogeochem. Cycles* **35** e2020GB006758
- Liu Y, Liu R and Chen J M 2012 Retrospective retrieval of long-term consistent global leaf area index (1981–2011) from combined AVHRR and MODIS data *J. Geophys. Res. Biogeosci.* **117** G4
- Mann H B 1945 Nonparametric tests against trend *Econometrica* **13** 245–59
- Manning C, Widmann M, Bevacqua E, Van Loon A F, Maraun D and Vrac M 2019 Increased probability of compound long-duration dry and hot events in Europe during summer (1950–2013) *Environ. Res. Lett.* **14** 094006
- Marino G P, Kaiser D P, Gu L and Ricciuto D M 2011 Reconstruction of false spring occurrences over the southeastern United States, 1901–2007: an increasing risk of spring freeze damage? *Environ. Res. Lett.* **6** 024015
- Martínez-Vilalta J, Poyatos R, Aguadé D, Retana J and Mencuccini M 2014 A new look at water transport regulation in plants *New Phytol.* **204** 105–15
- Menzel A, Yuan Y, Matiu M, Sparks T, Scheffinger H, Gehrig R and Estrella N 2020 Climate change fingerprints in recent European plant phenology *Glob. Change Biol.* **26** 2599–612
- Miguez-Macho G and Fan Y 2021 Spatiotemporal origin of soil water taken up by vegetation *Nature* **598** 624–8
- Mishra V, Thirumalai K, Singh D and Aadhar S 2020 Future exacerbation of hot and dry summer monsoon extremes in India *npj Clim. Atmos. Sci.* **3** 10
- Nemani R R, Keeling C D, Hashimoto H, Jolly W M, Piper S C, Tucker C J, Myneni R B and Running S W 2003 Climate-driven increases in global terrestrial net primary production from 1982 to 1999 *Science* **300** 1560–3
- Ogallo L A, Boulahya M S and Keane T 2000 Applications of seasonal to interannual climate prediction in agricultural planning and operations *Agric. For. Meteorol.* **103** 159–66
- Ogle K, Barber J J, Barron-Gafford G A, Bentley L P, Young J M, Huxman T E, Loik M E, Tissue D T and Cleland E 2015 Quantifying ecological memory in plant and ecosystem processes *Ecol. Lett.* **18** 221–35
- Ogle K, Liu Y, Vicca S and Bahn M 2021 A hierarchical, multivariate meta-analysis approach to synthesising global change experiments *New Phytol.* **231** 2382–94
- Park Williams A et al 2013 Temperature as a potent driver of regional forest drought stress and tree mortality *Nat. Clim. Change* **3** 292–7
- Peng S, Chen A, Xu L, Cao C, Fang J, Myneni R B, Pinzon J E, Tucker C J and Piao S 2011 Recent change of vegetation growth trend in China *Environ. Res. Lett.* **6** 044027
- Peng S, Piao S, Ciais P, Fang J and Wang X 2010 Change in winter snow depth and its impacts on vegetation in China *Glob. Change Biol.* **16** 3004–13
- Peñuelas J, Ciais P, Canadell J G, Janssens I A, Fernández-Martínez M, Carnicer J, Obersteiner M, Piao S, Vautard R and Sardans J 2017 Shifting from a fertilization-dominated to a warming-dominated period *Nat. Ecol. Evol.* **1** 1438
- Pfleiderer P, Menke I and Schleussner C-F 2019 Increasing risks of apple tree frost damage under climate change *Clim. Change* **157** 515–25

- Piao S *et al* 2014 Evidence for a weakening relationship between interannual temperature variability and northern vegetation activity *Nat. Commun.* **5** 5018
- Piao S, Wang X, Ciais P, Zhu B, Wang T and Liu J 2011 Changes in satellite-derived vegetation growth trend in temperate and boreal Eurasia from 1982 to 2006 *Glob. Change Biol.* **17** 3228–39
- Pohl F, Werban U, Kumar R, Hildebrandt A and Rebmann C 2023 Observational evidence of legacy effects of the 2018 drought on a mixed deciduous forest in Germany *Sci. Rep.* **13** 10863
- Poulter B *et al* 2015 Plant functional type classification for earth system models: results from the European space agency's land cover climate change initiative *Geosci. Model Dev.* **8** 2315–28
- Santini M, Noce S, Antonelli M and Caporaso L 2022 Complex drought patterns robustly explain global yield loss for major crops *Sci. Rep.* **12** 5792
- Santoro M, Kirches G, Wevers J, Boettcher M, Brockmann C, Lamarche C and Defourny P 2017 ESA. Land Cover CCI Product User Guide Version 2 *Tech. Rep.* (available at: maps.elie.ucl.ac.be/CCI/viewer/download/ESACCI-LC-Ph2-PUGv2_2.0.pdf)
- Seidl R *et al* 2017 Forest disturbances under climate change *Nat. Clim. Change* **7** 395–402
- Sharma S and Mujumdar P 2017 Increasing frequency and spatial extent of concurrent meteorological droughts and heatwaves in India *Sci. Rep.* **7** 15582
- Sjulgård H, Keller T, Garland G and Colombi T 2023 Relationships between weather and yield anomalies vary with crop type and latitude in Sweden *Agric. Syst.* **211** 103757
- Sweet L-B, Müller C, Anand M and Zscheischler J 2023 Cross-validation strategy impacts the performance and interpretation of machine learning models *Artif. Intell. Earth Syst.* **2** e230026
- Tominaga A, Ito A, Sugiura T and Yamane H 2022 How is global warming affecting fruit tree blooming? “Flowering (dormancy) disorder” in Japanese pear (*Pyrus pyrifolia*) as a case study *Front. Plant Sci.* **12** 787638
- Trnka M, Rötter R P, Ruiz-Ramos M, Kersebaum K C, Olesen J E, Žalud Z and Semenov M A 2014 Adverse weather conditions for European wheat production will become more frequent with climate change *Nat. Clim. Change* **4** 637–43
- van der Woude A M *et al* 2023 Temperature extremes of 2022 reduced carbon uptake by forests in Europe *Nat. Commun.* **14** 6218
- Vautard R *et al* 2023 Human influence on growing-period frosts like in early April 2021 in central France *Nat. Hazards Earth Syst. Sci.* **23** 1045–58
- Vogel J, Rivoire P, Deidda C, Rahimi L, Sauter C A, Tschumi E, van der Wiel K, Zhang T and Zscheischler J 2021 Identifying meteorological drivers of extreme impacts: an application to simulated crop yields *Earth Syst. Dyn.* **12** 151–72
- Walther S, Duveiller G, Jung M, Guanter L, Cescatti A and Camps-Valls G 2019 Satellite observations of the contrasting response of trees and grasses to variations in water availability *Geophys. Res. Lett.* **46** 1429–40
- Wang T *et al* 2018a Emerging negative impact of warming on summer carbon uptake in northern ecosystems *Nat. Commun.* **9** 5391
- Wang X, Wang T, Guo H, Liu D, Zhao Y, Zhang T, Liu Q and Piao S 2018b Disentangling the mechanisms behind winter snow impact on vegetation activity in northern ecosystems *Glob. Change Biol.* **24** 1651–62
- Webber H *et al* 2018 Diverging importance of drought stress for maize and winter wheat in Europe *Nat. Commun.* **9** 4249
- Wolf S *et al* 2016 Warm spring reduced carbon cycle impact of the 2012 US summer drought *Proc. Natl Acad. Sci.* **113** 5880–5
- Xiao C, Zaehle S, Yang H, Wigneron J-P, Schmulius C and Bastos A 2023 Land cover and management effects on ecosystem resistance to drought stress *Earth Syst. Dyn.* **14** 1211–37
- Yang Y, Maraun D, Ossó A and Tang J 2023 Increased spatial extent and likelihood of compound long-duration dry and hot events in China, 1961–2014 *Nat. Hazards Earth Syst. Sci.* **23** 693–709
- Yu X *et al* 2022 Contrasting drought legacy effects on gross primary productivity in a mixed versus pure beech forest *Biogeosciences* **19** 4315–29
- Zampieri M, Ceglar A, Dentener F and Toreti A 2017 Wheat yield loss attributable to heat waves, drought and water excess at the global, national and subnational scales *Environ. Res. Lett.* **12** 064008
- Zeng N, Zhao F, Collatz G J, Kalnay E, Salawitch R J, West T O and Guanter L 2014 Agricultural green revolution as a driver of increasing atmospheric CO₂ seasonal amplitude *Nature* **515** 394–7
- Zhang R, Ouyang Z-T, Xie X, Guo H-Q, Tan D-Y, Xiao X-M, Qi J-G and Zhao B 2016 Impact of climate change on vegetation growth in arid northwest of China from 1982 to 2011 *Remote Sens.* **8** 364
- Zhang Y, Sherstiukov A B, Qian B, Kokelj S V and Lantz T C 2018 Impacts of snow on soil temperature observed across the circumpolar north *Environ. Res. Lett.* **13** 044012
- Zhu L, Ives A R, Zhang C, Guo Y and Radeloff V C 2019 Climate change causes functionally colder winters for snow cover-dependent organisms *Nat. Clim. Change* **9** 886–93
- Zhu P *et al* 2022 The critical benefits of snowpack insulation and snowmelt for winter wheat productivity *Nat. Clim. Change* **12** 485–90
- Zhu Z, Piao S, Xu Y, Bastos A, Ciais P and Peng S 2017 The effects of teleconnections on carbon fluxes of global terrestrial ecosystems *Geophys. Res. Lett.* **44** 3209–18
- Zscheischler J *et al* 2014 Impact of large-scale climate extremes on biospheric carbon fluxes: an intercomparison based on MsTMIP data *Glob. Biogeochem. Cycles* **28** 585–600
- Zscheischler J *et al* 2020 A typology of compound weather and climate events *Nat. Rev. Earth Environ.* **1** 333–47
- Zscheischler J, Orth R and Seneviratne S I 2017 Bivariate return periods of temperature and precipitation explain a large fraction of European crop yields *Biogeosciences* **14** 3309–20